J. Membrane Biol. 129, 277–286 (1992)

The Journal of
Membrane Biology

Elevation of Cytosolic [Ca^{2+}] Due to Intracellular Ca^{2+} Release Retards Carbachol Stimulation of Divalent Cation Entry in Rat Parotid Gland Acinar Cells

Yukiharu Hiramatsu, Bruce J. Baum, and Indu S. Ambudkar
Clinical Investigations and Patient Care Branch, National Institute of Dental Research, National Institutes of Health, Bethesda, Maryland 20892

Summary. This study examines the activation of divalent cation entry into rat parotid gland acinar cells by using Mn^{2+} as a Ca^{2+} surrogate cation. Following muscarinic-cholinergic stimulation of dispersed parotid acini with carbachol (10 μM), the onset of internal Ca^{2+} release (cytosolic [Ca^{2+}], $[Ca^{2+}]_i$, increase) and the stimulation of Mn^{2+} entry (increase in fura2 quenching) are not simultaneously detected. $[Ca^{2+}]_i$ elevation, due to intracellular release, is detected almost immediately following carbachol addition and peak $[Ca^{2+}]_i$ increase occurs at 6.0 ± 0.8 sec. However, there is an interval (apparent lag) between carbachol addition and the detection of stimulated Mn^{2+} entry. This apparent lag is decreased from 26 ± 3.1 sec to 9.2 ± 1.5 sec when external Mn^{2+} ($[Mn^{2+}]_o$) is increased from 12.5 to 500 μM. It is not decreased further with increase in $[Mn^{2+}]_o$ from 500 μM to 1 mM (9.8 ± 2.1 sec), although both intracellular free Mn^{2+} and [Mn^{2+}-fura2]/[fura2] increase. Thus, at $[Mn^{2+}]_o$ <500 μM, the observed lag time is partially due to a limitation in the magnitude of Mn^{2+} entry. Furthermore, neither peak $[Ca^{2+}]_i$ nor the time required to reach peak $[Ca^{2+}]_i$ is significantly altered by $[Mn^{2+}]_o$ (12.5 μM to 1 mM). At every $[Mn^{2+}]_o$ tested (i.e., 12.5 μM–1 mM), the apparent lag is significantly greater than the time required to reach peak $[Ca^{2+}]_i$. However, when carbachol stimulation of the $[Ca^{2+}]_i$ increase is attenuated by loading the acini with the Ca^{2+} chelator, 2-bis(O-aminophenoxy)ethane-N,N,N′,N′-tetraacetate (BAPTA), there is no detectable lag in carbachol stimulation of Mn^{2+} entry (with 1 mM $[Mn^{2+}]_o$). Importantly, in BAPTA-loaded acini, carbachol stimulates Mn^{2+} entry via depletion of the internal Ca^{2+} pool and not via direct activation of other divalent cation entry mechanisms. Based on these results, we suggest that the apparent lag in the detection of carbachol stimulation of Mn^{2+} entry into parotid acinar cells is due to a retardation of Mn^{2+} entry by the initial increase in $[Ca^{2+}]_i$, due to internal release, which most likely occurs proximate to the site of divalent cation entry.

Key Words divalent cation entry · Mn^{2+} · $[Ca^{2+}]_i$ elevation · muscarinic-cholinergic receptor · parotid acinar cells

Introduction

Stimulation of calcium mobilizing receptors, such as the muscarinic-cholinergic receptor, in dispersed rat parotid acinar cells results in the release of Ca^{2+} from the intracellular agonist-sensitive store and the influx of Ca^{2+} from the external medium [3, 22, 26, 30, 31]. There are several studies which temporally correlate the generation of the second messenger, inositol 1,4,5-triphosphate (IP_3, a product of phosphatidylinositol 4,5-bisphosphate hydrolysis mediated by the activation of phospholipase C) with the release of intracellular Ca^{2+}, following stimulation of parotid cells by an agonist [1, 10, 14, 23]. However, the precise point at which Ca^{2+} entry commences during muscarinic stimulation of parotid acini, the characteristics of this Ca^{2+} entry pathway, and the mechanisms involved in its activation following stimulation are not yet clearly understood. Previous studies from several laboratories [12, 22–24, 34], utilizing Ca^{2+}-sensitive, fluorescent dyes, have shown that following carbachol stimulation of parotid acini there is an initial transient rise in $[Ca^{2+}]_i$ (due to intracellular Ca^{2+} release). This is followed by a lower, sustained elevation in $[Ca^{2+}]_i$, which is maintained during prolonged stimulation of the cells in a Ca^{2+}-containing medium. In the absence of external Ca^{2+}, the magnitude of the initial $[Ca^{2+}]_i$ peak remains unchanged, but the subsequent decline in $[Ca^{2+}]_i$ is accelerated and there is no sustained elevation in $[Ca^{2+}]_i$. These data [10, 12, 22, 24, 26, 34] suggest that Ca^{2+} entry is initiated after agonist-stimulated intracellular Ca^{2+} release and remains activated during prolonged stimulation.

Several recent studies with parotid acinar cells demonstrate that the depletion of Ca^{2+} from the internal stores stimulates Ca^{2+} entry, while its refill decreases Ca^{2+} entry [24, 34]. Studies with lacrimal gland and endothelial cells have indicated the involvement of inositol 1,3,4,5-tetrakisphosphate (IP_4) [20] and IP_3 in the activation of Ca^{2+} entry [11, 29]. However, studies with parotid gland cells suggest that inositol phosphate metabolites are most likely not directly involved in the activation of the

Ca^{2+} entry, but regulate the entry mechanism by altering the status of refill of the internal Ca^{2+} pool, i.e., depletion [5, 33]. Based on these studies, it can be suggested that Ca^{2+} entry should be activated as Ca^{2+} is released from the intracellular pool. Alternatively, a certain extent of depletion may be needed before Ca^{2+} entry can be activated. It has been proposed [13, 22] that the $[Ca^{2+}]$ in the internal pool is critical in the regulation of Ca^{2+} entry. The involvement of a soluble messenger between the internal Ca^{2+} pool and the plasma membrane has also been hypothesized [35].

In several types of cells, a temporal difference between the onset of intracellular Ca^{2+} release and the stimulation of Mn^{2+} (used as a Ca^{2+} surrogate) entry has been demonstrated [9, 15, 17, 32]. We had noted earlier that following carbachol stimulation of parotid acinar cells, the increase in quenching of fura2 due to Mn^{2+} entry did not coincide with the onset of internal Ca^{2+} release [24]. This apparent lag in the stimulation of divalent cation entry can be due to several factors: (i) actual delay in the activation of divalent cation entry, (ii) competition between Ca^{2+} and Mn^{2+} for intracellular fura2, (iii) limitation of the amount of Mn^{2+} entering the cell immediately following stimulation, and (iv) inhibition of divalent cation entry due to the initial elevation of $[Ca^{2+}]_i$. In this study we have addressed these possibilities, and our results suggest that the apparent lag in the stimulation of Mn^{2+} (and Ca^{2+}) entry following muscarinic receptor stimulation in parotid acini is not due to an actual delay in the activation of the entry mechanism. Rather, it is due to a retardation of Mn^{2+} entry by the initial high level of $[Ca^{2+}]_i$ induced as a result of intracellular Ca^{2+} release.

Materials and Methods

The animals used in this study were male Wistar rats (Harlan Sprague-Dawley) with an average weight of 200–300 g. The rats were caged in temperature controlled, independently ventilated enclosures and allowed chow (NIH Purina) and water *ad libitum*. Collagenase (CLSPA; sp at 300 U/mg) was purchased from Cooper Biochemical. Carbamylcholine chloride (carbachol), atropine sulphate, hyaluronidase (Type II), bovine serum albumin (BSA), and lima bean trypsin inhibitor (Type II-L) were from Sigma. Fura2/AM and BAPTA/AM were obtained from Calbiochem and stored at −70°C as 5 or 50 mM stock solutions, respectively, in dimethylsulfoxide. Ca^{2+} and Mg^{2+}-free Hank's balanced salt solution (HBSS) was purchased from GIBCO. All other reagents were of the highest chemical grade available.

Rats were killed between 9–12 a.m. by cardiac puncture following ether anesthesia. Enzymatically dispersed acini were prepared as described [2] using collagenase and hyaluronidase in the HBSS buffered with HEPES (33 mM, pH 7.4) containing 1.28 mM $CaCl_2$, 1 mM $MgSO_4$, and 0.01% BSA (HBSS medium). This medium was used in all subsequent procedures. After dispersion the cells were washed and resuspended in the same medium with lima bean trypsin inhibitor (2 mg/10 ml). 2 μM fura2/AM, with or without 50 μM BAPTA/AM, was added and the cells were incubated for 45 min at 30°C, following which they were washed and kept at 30°C until used with gassing every 20 min (95% O_2/5% CO_2).

Fura2 fluorescence was measured in an SLM 8000 spectrofluorimeter with the excitation and emission band passes adjusted to 4 nm. Before each assay the cells were gently pelleted at 400 × *g* and resuspended in fresh Ca^{2+}-free medium. For each assay 1.5 ml of cell suspension was gently stirred in a cuvette maintained at 37°C. Excitation wavelengths were 340 and 360 nm and emission was set at 510 nm.

To estimate intracellular-free or fura2-bound Ca^{2+} or Mn^{2+}, we used the equations previously described by Foder et al. [7], except that in our calculations we assumed that the dye leak was negligible during the course of the assay (about 200 sec). We have experimentally verified this using DTPA (*data not shown*).

$$[Ca^{2+}]_i = \frac{K_{Ca}[(F_m - F_{min}) - (F_{m_0} - F_m)[Mn^{2+}]_i/K_{Mn}]}{F_{m_0} - F_m} \quad (1)$$

$$[Mn^{2+}]_i = K_{Mn}(1 + [Ca^{2+}]_i/K_{Ca}) \frac{F' - F'_m}{F'_m - F'_{m_0}} \quad (2)$$

These equations were arranged as follows:

$$[Ca^{2+}]_i = \frac{K_{Ca}\left[(F_m - F_{min}) - \dfrac{(F_{m_0} - F_m)(F' - F'_m)}{F'_m - F'_{m_0}}\right]}{(F_{max} - F_m) + \dfrac{(F_{m_0} - F_m)(F' - F'_m)}{F'_m - F'_{m_0}}} \quad (3)$$

$$[Mn^{2+}]_i = \frac{K_{Mn}\dfrac{(F_{max} - F_{min})(F' - F'_m)}{F'_m - F'_{m_0}}}{(F_{max} - F_m) + \dfrac{(F_{m_0} - F_m)(F' - F'_m)}{F'_m - F'_{m_0}}} \quad (4)$$

And total intracellular $[Mn^{2+}]$ ($[Mn]_i$) was calculated as follows:

$$[Mn]_i = \left[1 + \frac{[fura2]}{K_{Mn}(1 + [Ca^{2+}]_i/K_{Ca}) + [Mn^{2+}]_i}\right][Mn^{2+}]_i. \quad (5)$$

The concentration of intracellular fura ([fura2]) was assumed to be much higher than $[Mn^{2+}]_i$. Based on this assumption, the former equation was arranged as follows:

$$[Mn]_i/[fura2] \fallingdotseq \frac{[Mn^{2+}]_i}{K_{Mn}(1 + [Ca^{2+}]_i/K_{Ca}) + [Mn^{2+}]_i}. \quad (6)$$

The conditions used to obtain the various fluorescence values were: F (340 nm), F' (360 nm), F_m (340 nm, Mn^{2+}), F'_m (360 nm, Mn^{2+}), F_{m_0} (340 nm, Mn^{2+}, Triton X-100), F'_{m_0} (360 nm, Triton X-100, Mn^{2+}), F_{max} (340 nm, Triton X-100, $CaCl_2$ 200 μM, Mn^{2+}, DTPA 2 mM), F_{min} (340 nm, Triton X-100, Ca^{2+} 200 μM, Mn^{2+},

EGTA 10 mM, DTPA 2 mM. Note that DTPA addition does not affect F_{max} in the absence of Mn^{2+}).

Results

Fluorescence of fura2-loaded, dispersed parotid acini was measured with dual excitation wavelengths of 340 and 360 nm to obtain Ca^{2+}-sensitive and Ca^{2+}-insensitive fluorescence changes simultaneously. In the absence of extracellular Mn^{2+} or Ca^{2+}, carbachol (10 μM) induces a rapid rise in $[Ca^{2+}]_i$ (detected as an increase in fura2 fluorescence when excitation is at 340 nm) from a resting level of about 120 nM to a transient peak of about 430 nM, which is reached at about 6 sec after stimulation (further addressed below). We have shown earlier that this initial peak $[Ca^{2+}]_i$ is similar to that obtained in the presence of extracellular Ca^{2+} (1.28 mM), and represents intracellular Ca^{2+} release [10, 26]. In the presence of 50 μM extracellular Mn^{2+}, fura2 fluorescence with both 340 and 360 nm excitation gradually declines, even in the absence of the agonist (Fig. 1*A* and *B*). When carbachol is added, a sharp $[Ca_{2+}]_i$ increase is seen at the Ca^{2+}-sensitive excitation wavelength (Fig. 1*A*), which rapidly decreases to below resting levels. In the experiment depicted in Fig. 1*A* peak $[Ca^{2+}]_i$ was calculated to be 360 nM, which was not different from that obtained in control cells (no Mn^{2+}, *see below* and Fig. 4). At 360 nm excitation (Fig. 1*B*), carbachol induces about twofold increase, over basal, in fura2 fluorescence-quench rate, which is due to the stimulation of Mn^{2+} entry [24, 25]. However, this increase in fura2 quenching does not occur immediately after the addition of agonist. In this particular experiment stimulation of Mn^{2+} entry was detected 24 sec after carbachol addition (*see* Fig. 2 for additional data). Conversely, the increase in fura2 fluorescence due to internal Ca^{2+} release begins almost immediately (within 2 sec) and peak $[Ca^{2+}]_i$ increase is detected at 6 sec. It should be noted that there is no such lag in the detection of fura2 quenching upon Mn^{2+} addition to either basal cells or Ca^{2+}-depleted cells [22, 25]. Thus, the apparent lag in the stimulation of Mn^{2+} entry following carbachol addition is not due to mixing time or diffusional limitations.

This apparent lag between cell stimulation and the detection of agonist-stimulated Mn^{2+} entry could be a result of a delay in the activation of divalent cation entry. However, as mentioned above, a number of other factors could also account for the lag. One possible factor could be a competition between $[Mn^{2+}]_i$ and $[Ca^{2+}]_i$ for fura2, since, following carbachol stimulation, at the time when Mn^{2+} entry appears to be stimulated, $[Ca^{2+}]_i$ is substantially elevated. Thus, in spite of the higher affinity of Mn^{2+} for fura2 [18], fura2 quenching achieved by Mn^{2+} may not be detectable until the peak $[Ca^{2+}]_i$ declines. Alternatively, it can be suggested that since the rate of Mn^{2+} entry gradually increases following carbachol stimulation (i.e., as Ca^{2+} pool is depleted), the amount of Mn^{2+} initially entering the cell is not sufficient to produce a detectable quench of fura2. In either case, the magnitude of Mn^{2+} entry can be expected to influence the lag time.

We have assessed these possibilities by examining the effect of varying $[Mn^{2+}]_o$ on the apparent lag detected between the addition of carbachol and an increase in fura2 quenching (Fig. 1*B–E*) or peak $[Ca^{2+}]_i$ increase (*see* Fig. 4). Based on earlier studies [21, 26], which have shown that the magnitude of Ca^{2+} entry into parotid acinar cells is dependent on $[Ca^{2+}]_o$, $[Mn^{2+}]_o$ was varied between 12.5 μM and 1 mM. Representative patterns of basal and carbachol-stimulated fura2 quenching with $[Mn^{2+}]_o$ 50 μM, 200 μM, 500 μM, and 1 mM are shown in Fig. 1*B–E*. The lag times shown in the figure are given in the legend and summarized from seven to eight similar experiments in Fig. 2. A significant, sharp decrease in the lag time is observed with increasing $[Mn^{2+}]_o$, 26 ± 3.1 sec at 12.5 μM to 9.2 ± 1.5 sec at 500 μM. Increasing $[Mn^{2+}]_o$, from 500 μM to 1 mM, does not decrease the lag time further (9.2 ± 1.5 and 9.8 ± 1.2 sec, respectively). It is important to note that the increase in $[Mn^{2+}]_o$ did not significantly change the time required to reach peak $[Ca^{2+}]_i$ (Fig. 2) or the extent of the initial increase in $[Ca^{2+}]_i$ induced by carbachol (discussed below). Further, the addition of DTPA to chelate extracellular Mn^{2+}, either simultaneously with carbachol, or 2.8 and 5.6 sec after carbachol, did not affect peak $[Ca^{2+}]$ (*data not shown*). These results indicate that upon carbachol stimulation of parotid acini, augmentation of Mn^{2+} entry occurs subsequent to the initial internal Ca^{2+} release.

The data shown in Fig. 2 suggest that at $[Mn^{2+}]_o$ <500 μM, the apparent lag in carbachol stimulation of Mn^{2+} entry is partially due to limitations in the magnitude of Mn^{2+} entry, while at higher $[Mn^{2+}]_o$ (500 μM–1 mM), it appears to be independent of $[Mn^{2+}]_o$. It is possible that at $[Mn^{2+}]_o$ >500 μM there is a saturation of the Mn^{2+} entry process. To estimate the magnitude of Mn^{2+} entry, we used the equations described by Foder et al. ([7], *see* Materials and Methods for details) to calculate intracellular free $[Mn^{2+}]$ ($[Mn^{2+}]_i$), $[Mn^{2+}$-fura2]/[fura2], $[Ca^{2+}]_i$, and $[Ca^{2+}$-fura2]/[fura2] in parotid cells at different $[Mn^{2+}]_o$. The total amount of Mn^{2+} in the cells ($[Mn]_i$), including both free and fura2-bound forms, represents Mn^{2+} entry. Figure 3 shows the change in $[Mn^{2+}]_i$ (Fig. 3*A*) and $[Mn^{2+}$-fura2]/[fura2] (Fig.

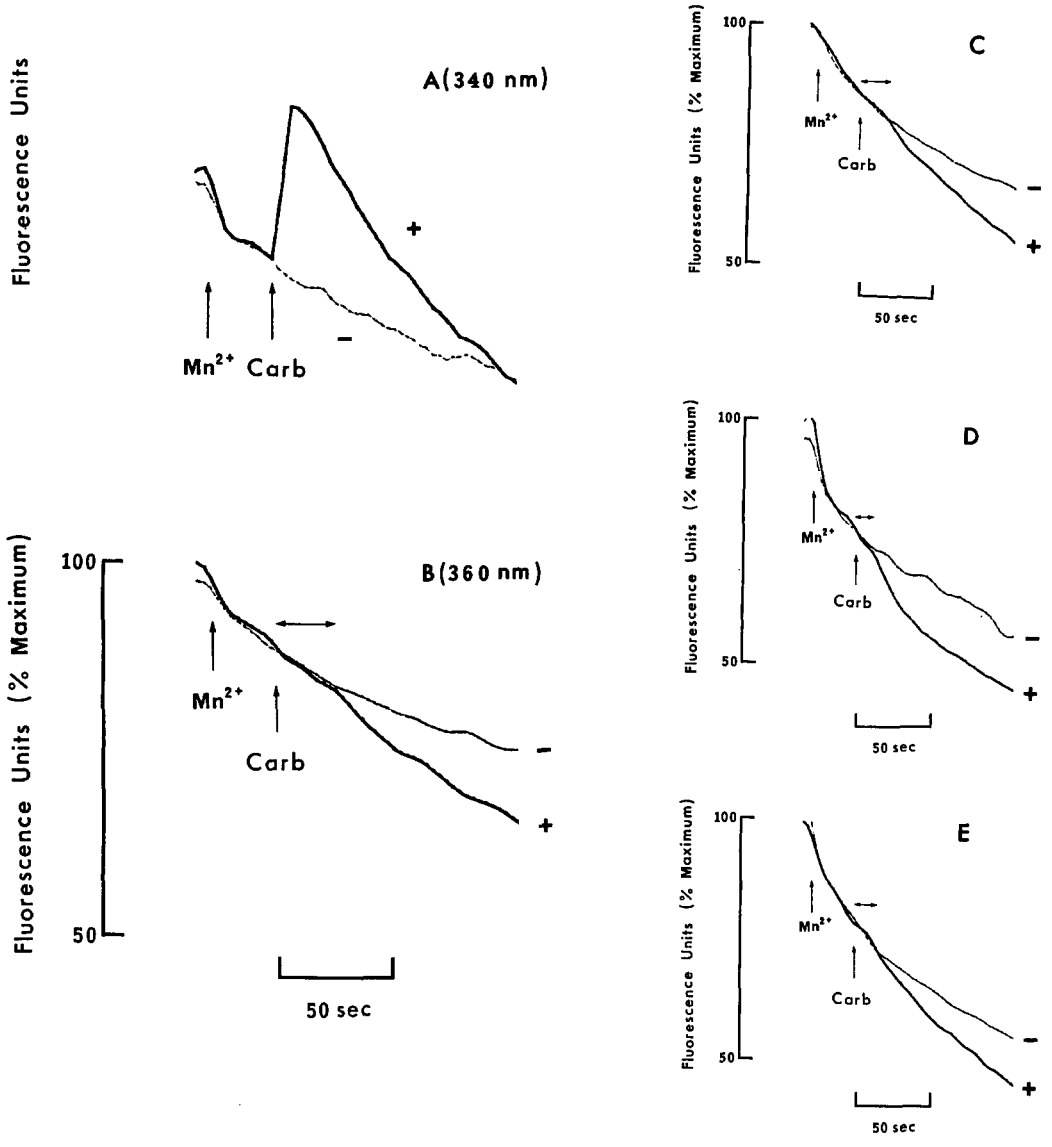

Fig. 1. Detection of an apparent lag in carbachol-stimulation of Mn^{2+} entry in parotid acini. Cells, prepared and loaded with fura2 as described in Materials and Methods, were washed and resuspended in Ca^{2+}-free HBSS medium. Fura2 fluorescence with excitation at 340 nm (*A*) and Mn^{2+}-dependent quenching of fura2 fluorescence with excitation at 360 nm (*B–E*) were measured simultaneously, either in the presence (+) or absence (−) of 10 μM carbachol (*Carb*). Addition of 50 μM $MnCl_2$ (Mn^{2+}) and carbachol is shown by arrows. (*A*) Resting and peak $[Ca^{2+}]_i$ calculated, as described in Materials and Methods [7], for the trace shown in *A* were 134 and 360 nM, respectively, which are not significantly different from the $[Ca^{2+}]_i$ obtained in control cells with no Mn^{2+} (for further details *see* Fig. 4). The patterns of fura2 quenching in the presence and absence of carbachol with various $[Mn^{2+}]_o$ (50 μM, 200 μM, 500 μM and 1 mM) are shown in *B–E*. The lag times at these $[Mn^{2+}]_o$ (25.2, 18.2, 11.2, and 12.6 sec, respectively) have been shown by horizontal arrows and represent the time between carbachol addition and the intercept of basal and stimulated fura2 quenching. The data are representative of at least seven to eight experiments each with a different cell preparation (*also see* Fig. 2).

3*B*) in the cells before stimulation (dashed line) and 30 sec after carbachol stimulation (solid line) at different $[Mn^{2+}]_o$. With increasing $[Mn^{2+}]_o$ both $[Mn^{2+}]_i$ and $[Mn^{2+}$-fura2]/[fura2] increase. However, with carbachol stimulation, there is a much greater increase in $[Mn]_i$. The data show that Mn^{2+} entry into parotid acini is not saturated at $[Mn^{2+}]_o$ between 500 μM and 1 mM. Thus the lag (about 9.8 sec) observed with 1 mM $[Mn^{2+}]_o$ cannot be accounted for by a limitation in the magnitude of Mn^{2+} entry.

Figure 4*A* shows the pattern of $[Ca^{2+}]_i$ as a function of time after carbachol stimulation of cells in a Ca^{2+}-free medium containing 50 μM or 1 mM Mn^{2+}. $[Ca^{2+}]_i$ in cells suspended in media containing Mn^{2+} was calculated based on the equations described by

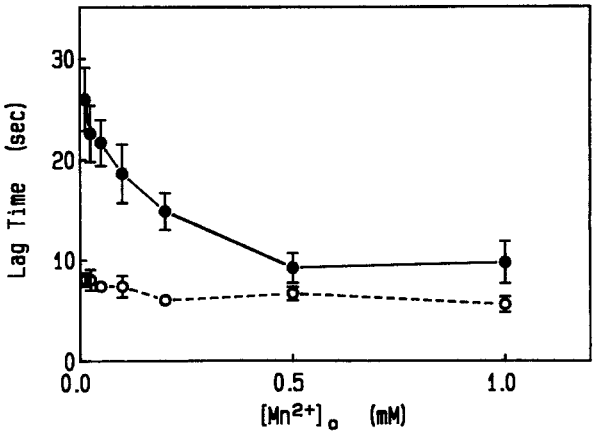

Fig. 2. Effect of $[Mn^{2+}]_o$ on the apparent lag in carbachol stimulation of Mn^{2+} entry and on the time to reach peak $[Ca^{2+}]_i$ increase. Experimental conditions were similar to those described for Fig. 1. The time taken for peak $[Ca^{2+}]_i$ increase (dashed line) represents the interval between carbachol (10 μM) addition and peak increase in fura2 fluorescence due to internal Ca^{2+} release. The lag time for stimulation of Mn^{2+} entry (solid line) was determined as described previously [28, 29]. The values shown are mean ± SEM obtained from seven to eight experiments, each with a different cell preparation.

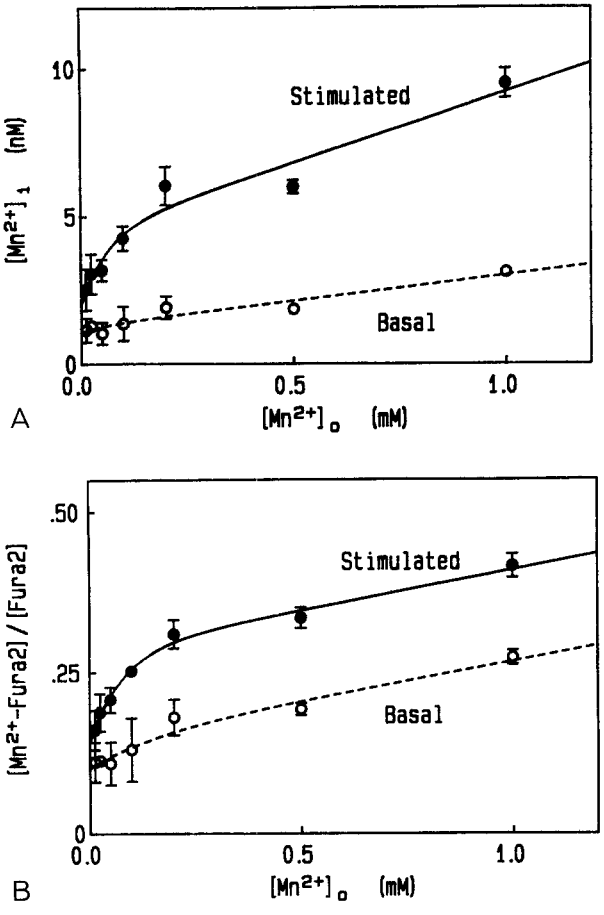

Fig. 3. Effect of $[Mn^{2+}]_o$ on $[Mn^{2+}]_i$ and [Mn^{2+}-fura2]/[fura2] in carbachol-stimulated parotid acini. $[Mn^{2+}]_i$ (*A*) and [Mn^{2+}-fura2]/[fura2] (*B*) were calculated as described in Materials and Methods. The various $[Mn^{2+}]_o$ are indicated in the figure. Values were calculated for the same cells either 2 sec before carbachol addition (dashed line) or 30 sec after carbachol addition (solid line). The data shown are mean ± SEM from three experiments, each with different cell preparations.

Foder et al. (*see above*). A similar pattern of $[Ca^{2+}]_i$ is seen at all the concentrations of Mn^{2+} tested (12.5 μM–1 mM), although all the data are not shown here. Both resting and peak $[Ca^{2+}]_i$ values calculated from these experiments are not significantly different from each other (shown in Fig. 4*B*). Average peak $[Ca^{2+}]_i$ is 436 ± 18 nM, a 310 ± 17 nM increase above the average resting value, 125 ± 4 nM. The pattern of [Ca^{2+}-fura2]/[fura2] following carbachol stimulation of acini is also similar at all the $[Mn^{2+}]_o$ tested (between 12.5 μM to 1 mM, *data not shown*). The lack of quenching of the initial $[Ca^{2+}]_i$ peak increase at high $[Mn^{2+}]_o$ strongly suggests that there is no detectable Mn^{2+} entry during internal Ca^{2+} release.

The data presented above show that the apparent lag in carbachol stimulation of Mn^{2+} entry temporally coincides with the initial phase of $[Ca^{2+}]_i$ increase due to internal Ca^{2+} release. To assess whether this $[Ca^{2+}]_i$ elevation directly affects Mn^{2+} entry, and accounts for the apparent lag, we loaded the cells with the permeant Ca^{2+} chelator, BAPTA, and then examined carbachol stimulation of Mn^{2+} entry into the BAPTA-loaded cells. The data are shown in Figs. 5 and 6. Upon carbachol stimulation of BAPTA-loaded cells the initial increase in $[Ca^{2+}]_i$ is attenuated due to increased intracellular Ca^{2+} buffering (Fig. 5). Similarly, BAPTA loading also appears to buffer intracellular $[Mn^{2+}]$ since the basal rate of fura2 quenching due to Mn^{2+} entry (with 1 mM $[Mn^{2+}]_o$, Fig. 6*A*) is low compared to that in control cells without BAPTA (*see* Fig. 1). Despite this buffering, upon carbachol addition there is a sharp increase in fura2 quenching. Importantly, there is no detectable lag between the addition of carbachol and the increase in the rate of fura2 quenching. These data strongly suggest that the initial elevation in $[Ca^{2+}]_i$ induced by carbachol retards divalent cation entry.

It is also possible that BAPTA loading itself causes the depletion of the internal Ca^{2+} pool, which then facilitates subsequent carbachol stimulation of Mn^{2+} entry, directly via a receptor or second messenger operated mechanism. Such a situation has been recently reported by Kass et al. [17] in the case of vasopressin stimulation of hepatocytes. To demonstrate that the stimulation of Mn^{2+} entry in

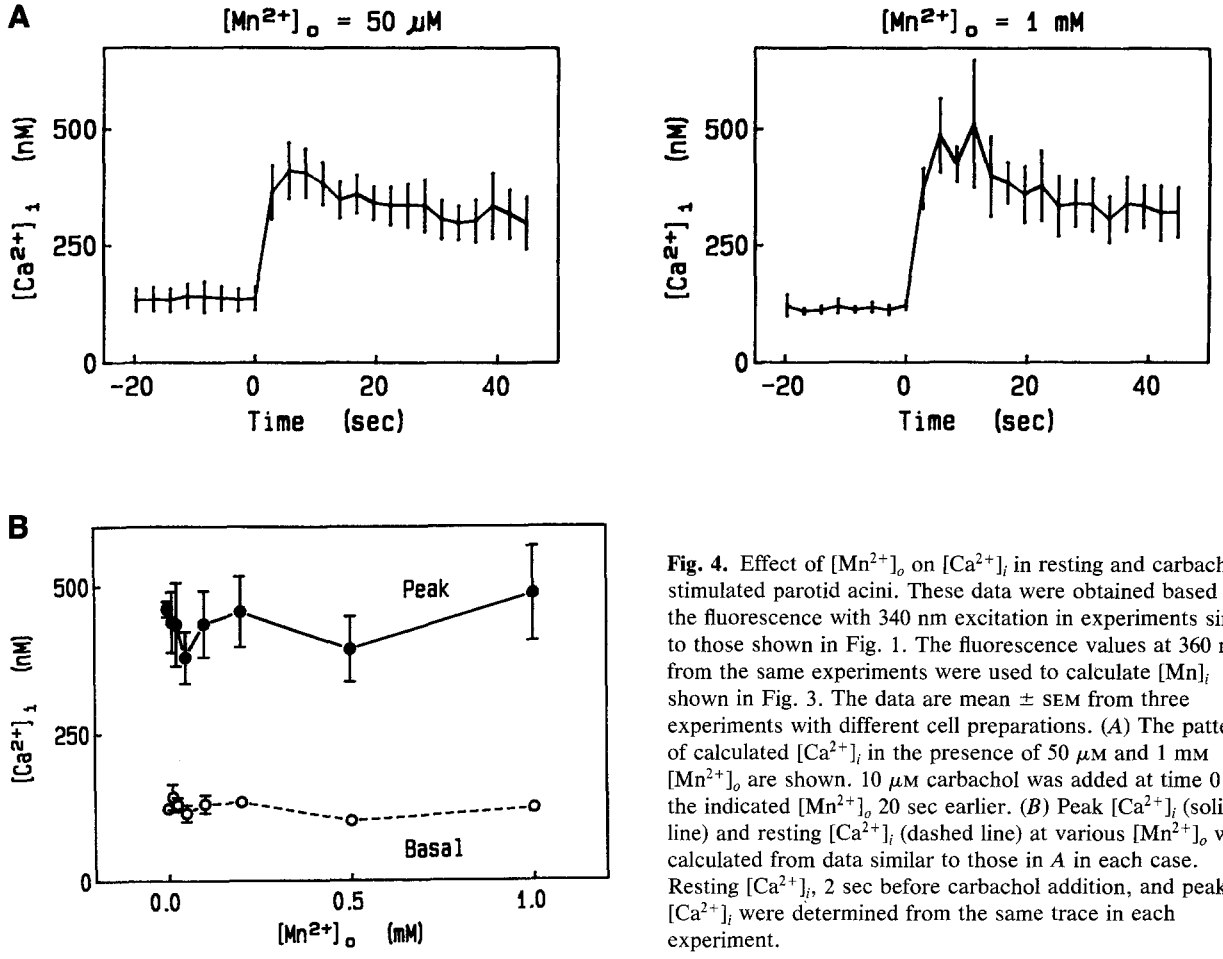

Fig. 4. Effect of $[Mn^{2+}]_o$ on $[Ca^{2+}]_i$ in resting and carbachol-stimulated parotid acini. These data were obtained based on the fluorescence with 340 nm excitation in experiments similar to those shown in Fig. 1. The fluorescence values at 360 nm from the same experiments were used to calculate $[Mn]_i$ shown in Fig. 3. The data are mean ± SEM from three experiments with different cell preparations. (*A*) The patterns of calculated $[Ca^{2+}]_i$ in the presence of 50 μM and 1 mM $[Mn^{2+}]_o$ are shown. 10 μM carbachol was added at time 0 and the indicated $[Mn^{2+}]_o$ 20 sec earlier. (*B*) Peak $[Ca^{2+}]_i$ (solid line) and resting $[Ca^{2+}]_i$ (dashed line) at various $[Mn^{2+}]_o$ were calculated from data similar to those in *A* in each case. Resting $[Ca^{2+}]_i$, 2 sec before carbachol addition, and peak $[Ca^{2+}]_i$ were determined from the same trace in each experiment.

BAPTA-loaded parotid acinar cells is coupled to the depletion of the internal Ca^{2+} pool, cells were first depleted of internal Ca^{2+}, by stimulation with carbachol in Ca^{2+}-free medium for 10 min, and then loaded with BAPTA. Mn^{2+} entry into these Ca^{2+}-depleted, BAPTA-loaded cells is higher than in unstimulated BAPTA-loaded cells (*compare* lighter lines in Fig. 6*A* and *B*), a result consistent with the capacitative activation of divalent cation entry. Upon restimulation of these cells with carbachol, there is no further increase either in Mn^{2+} entry (Fig. 6*B*, bolder line) or $[Ca^{2+}]_i$ (*not shown*). That this lack of response is not due to a desensitization of carbachol-stimulated Ca^{2+} mobilization is shown in Fig. 6*C*. When Ca^{2+}-depleted, BAPTA-loaded cells are further incubated in 10 mM Ca^{2+}-containing medium (for 10 min) to refill the internal Ca^{2+} pool, the basal rate of Mn^{2+} entry is decreased to levels similar to that in control, BAPTA-loaded cells (*compare* lighter lines in Fig. 6*A* and *C*). Furthermore, similar to control BAPTA-loaded cells, the addition of carbachol induces an immediate increase in the rate of Mn^{2+} entry (Fig. 6*C*, bolder line). An attenuated $[Ca^{2+}]_i$ increase (*not shown*) similar to that induced by carbachol in control cells (Fig. 5) is observed.

Discussion

Several recent studies have supported the proposal previously made by Putney, that intracellular Ca^{2+} release stimulates Ca^{2+} entry into rat parotid acinar cells and that the extent of pool depletion determines the magnitude of Ca^{2+} entry [5, 24, 26, 31, 33, 34]. Based on this "capacitative" regulation of Ca^{2+} entry, intracellular Ca^{2+} release should either coincide with or precede Ca^{2+} entry. Data obtained from intracellular Ca^{2+} measurements, which have been reported by several laboratories including ours, indicate that Ca^{2+} entry is most likely initiated after Ca^{2+} release has occurred. This suggestion is also supported by our observation, using Mn^{2+} to assess Ca^{2+} entry more directly, that stimulation of Mn^{2+} entry does not coincide with the stimulation of intracellular Ca^{2+} release [24].

In contrast to the stimulation of intracellular

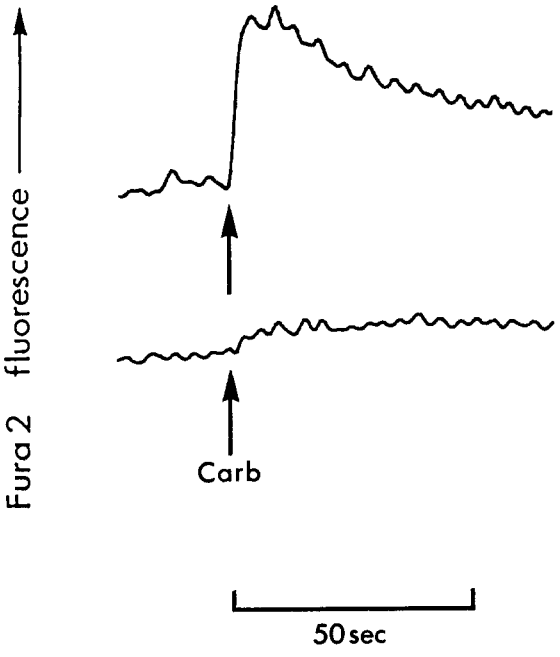

Fig. 5. Attenuation of carbachol-stimulated $[Ca^{2+}]_i$ increase in BAPTA-loaded parotid acini. Parotid acini were loaded with BAPTA as described in Materials and Methods. 10 μM carbachol was added where indicated to control (top trace) or BAPTA-loaded (bottom trace) acini. Fura2 fluorescence was monitored with excitation at 340 nm. Peak $[Ca^{2+}]_i$ calculated for control cells is given in the text. $[Ca^{2+}]_i$ in fura2 and BAPTA-loaded cells could not be calculated. The data are representative of at least five to seven experiments, each with a different cell preparation.

Ca^{2+} release, observed almost immediately upon cell stimulation, an apparent lag is detected in the stimulation of Mn^{2+} entry by carbachol and, as pointed out earlier in this paper, at least four factors could account for this lag. In this study we have assessed the role of these four factors and have identified a possible mechanism that could account for the observed lag in the stimulation of Mn^{2+} entry by carbachol. We have demonstrated that at low $[Mn^{2+}]_o$ this lag is partially determined by the magnitude of Mn^{2+} entry, due to either a competition of $[Ca^{2+}]_i$ and $[Mn^{2+}]_i$ for intracellular fura2 or a limitation in the amount of Mn^{2+} initially entering the cell. At higher $[Mn^{2+}]_o$ (0.5–1 mM), a lag of about 9.5 sec persists in the detection of stimulated Mn^{2+} entry, which is independent of $[Mn^{2+}]_o$. We have also shown that peak $[Ca^{2+}]_i$ is not altered by manipulations of external $[Mn^{2+}]_o$. Even with $[Mn^{2+}]_o$ close to physiological levels of Ca^{2+}, there is no quenching of the initial increase in fura2 fluorescence due to intracellular Ca^{2+} release. Thus, we can rule out the possibility that the lag is due to (i) competition between Mn^{2+} and Ca^{2+} for intracellular fura2 and (ii) limitation in the amount of Mn^{2+}

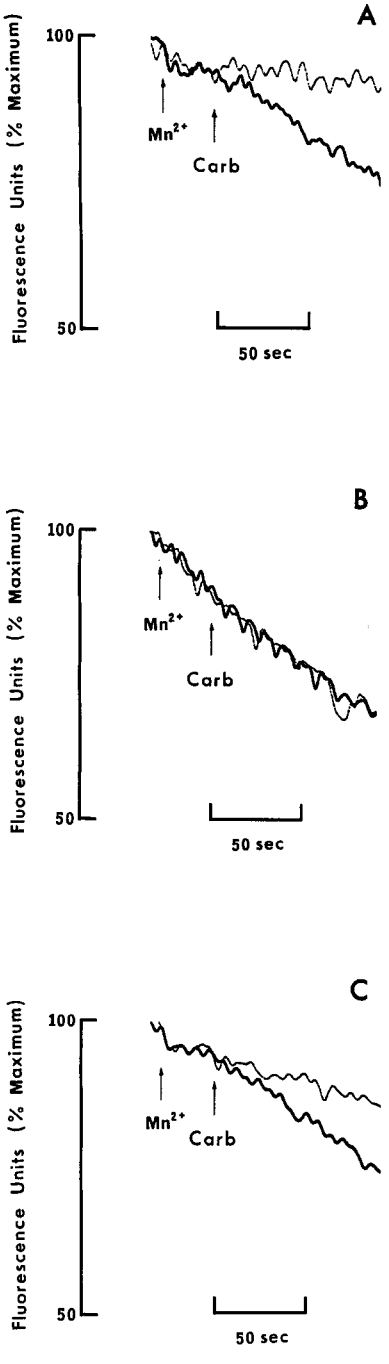

Fig. 6. Effect of BAPTA loading on carbachol stimulation of Mn^{2+} entry into parotid acinar cells. Control cells (*A*) and Ca^{2+}-depleted cells (*B*) were loaded with BAPTA as described in Materials and Methods (cells were Ca^{2+} depleted by carbachol stimulation for 10 min in Ca^{2+}-free HBSS). (*C*) Ca^{2+}-depleted, BAPTA loaded cells were further incubated with 10 mM Ca^{2+} for 10 min (refilled cells). All cells were washed and suspended in Ca^{2+}-free HBSS before the experiment. 1 mM Mn^{2+} and 10 μM carbachol (bolder line) were added as indicated by arrows. Carbachol was not added in the case of traces shown by lighter lines. Fluorescence was determined with excitation at 360 nm. The data represent five to six experiments with different cell preparations.

entering the cell. Based on these data, it would appear, as suggested previously, that intracellular Ca^{2+} release precedes Ca^{2+} (or Mn^{2+}) entry. However, we have shown that in BAPTA-loaded cells there is no detectable lag in the stimulation of Mn^{2+} entry following carbachol addition. Importantly, in these BAPTA-loaded cells, stimulation of Mn^{2+} entry by carbachol is dependent on the release of the internal Ca^{2+} pool. Based on these data we suggest that the persistent lag detected in the stimulation of Mn^{2+} entry by carbachol is a result of the retardation of divalent cation entry by the initial transient increase in $[Ca^{2+}]_i$ and not due to an actual delay in the activation of the entry mechanism. Consistent with this suggestion, Loessberg et al. [19] have recently shown that, during Ca^{2+} oscillations in pancreatoma cells (AR42J), a decrease in $[Ca^{2+}]_i$ is correlated with an increase in Mn^{2+} entry. They have also suggested a negative regulation of divalent cation entry by elevated $[Ca^{2+}]_i$.

There are a number of earlier reports from studies with parotid and other cells which suggest that $[Ca^{2+}]_i$ does not directly affect Ca^{2+} entry. These are mostly based on observations that Ca^{2+} entry is independent of changes in $[Ca^{2+}]_i$ [3, 12, 22, 26, 31]. For example, Ca^{2+} entry is initiated when $[Ca^{2+}]_i$ is high (i.e., at peak) and remains activated even after $[Ca^{2+}]_i$ decreases, as seen after prolonged stimulation of parotid acini by carbachol in Ca^{2+}-containing or Ca^{2+}-free media. However, these earlier proposals do not take into account localized changes in $[Ca^{2+}]_i$ recently observed in several cell types [4, 16]. Evidence for such a localized increase in $[Ca^{2+}]_i$ in rat parotid acini has been recently provided by Dissing et al. [6]. Using fluorescence imaging of single parotid acinar cells, these investigators have shown that the initial elevation in $[Ca^{2+}]_i$ due to agonist-induced intracellular Ca^{2+} release, occurs near the basolateral plasma membrane. Elevated $[Ca^{2+}]_i$ is maintained in this region for about 10 sec and then, due to intracellular Ca^{2+} regulatory mechanisms, $[Ca^{2+}]_i$ in this region dissipates and becomes more homogeneously distributed in the cell. In an earlier report Foskett et al. [8] have also suggested that, following carbachol stimulation of parotid acini, there are $[Ca^{2+}]_i$ changes localized to the basolateral region of the parotid acinar cell. In aggregate, these observations indicate that the region of the parotid cell in which the initial increase of $[Ca^{2+}]_i$ occurs and into which Ca^{2+} entry is mediated is located near the basolateral plasma membrane. Contradictory to these findings, initial $[Ca^{2+}]_i$ increase has been detected in the luminal region of pancreatic acinar cells [16]. However, the findings described above with rat parotid acinar cells are consistent with the suggestion we have made here that a $[Ca^{2+}]_i$ increase in the region of Mn^{2+} entry retards Mn^{2+} influx and can account for the lag typically observed in the stimulation of Mn^{2+} entry by carbachol. It is possible that as $[Ca^{2+}]_i$ in this region recedes, due to intracellular Ca^{2+} regulation (as observed by Dissing et al. [6]), Mn^{2+} entry is increased. Alternatively, there are well-documented feedback effects of Ca^{2+} on IP_3-stimulated internal Ca^{2+} release [27, 28]. Thus, it is possible that the observed lag in the stimulation of Mn^{2+} entry by carbachol may be a result of transient inhibition of internal Ca^{2+} release and refill of the internal Ca^{2+} pool. Further studies will be required to test this possibility.

The present study demonstrates that in rat parotid acinar cells carbachol stimulation of divalent cation entry temporally coincides with and is a result of internal Ca^{2+} release. There are several recent reports that show that Ca^{2+} entry into parotid acinar cells can be activated in the absence of receptor stimulation, increased phosphoinositide turnover, or IP_4 formation [5, 26, 33] and earlier studies that showed that Ca^{2+} entry remains activated even after carbachol-induced signalling is terminated [3, 24, 31, 34]. Additionally, we have previously reported that the extent of Mn^{2+} entry into these cells depends on the refill status of the internal agonist-sensitive Ca^{2+} pool [24]. In aggregate, these studies provide convincing evidence for the regulation of divalent cation entry into rat parotid acinar cells by the depletion of the internal Ca^{2+} pool. The molecular mechanism(s) involved in detecting and signalling the depletion of the internal Ca^{2+} store to the plasma membrane in order to gate the Ca^{2+} entry process has not yet been described. It has been suggested [35] that the $[Ca^{2+}]$ in the internal pool is signalled to the plasma membrane via a second messenger, which is released from the internal pool and diffuses to the site of Ca^{2+} influx. Alternatively, it has been proposed that there may be a physical interaction between the pool membrane and the plasma membrane, which is sensitive to the $[Ca^{2+}]$ in the pool [13]. Presently, there are no data that provide evidence for either mechanism.

We have previously shown that, in addition to Ca^{2+} pool depletion, divalent cation entry into rat parotid acinar cells is modulated by the membrane potential, via effects on the driving force for Ca^{2+} entry [25]. The present data show that $[Ca^{2+}]_i$ also regulates Ca^{2+} entry. $[Ca^{2+}]_i$, like membrane potential, could alter divalent cation influx via effects on the electrochemical potential or, alternatively, it could have a more direct effect on the Ca^{2+} influx pathway [11]. Thus, the present data, together with previous reports [27, 28], show that

the two main Ca^{2+} influx pathways into the cytosol, i.e., IP_3-mediated internal Ca^{2+} release and extracellular Ca^{2+} entry, are inhibited in a feedback manner by $[Ca^{2+}]_i$. This suggests the presence of an extremely effective mechanism for limiting increases in $[Ca^{2+}]_i$ in parotid cells. Although further studies are required to resolve the mechanism by which $[Ca^{2+}]_i$ regulates divalent cation entry, a physiological implication of our findings is that, in addition to the suggested role of $[Ca^{2+}]$ in the internal pool in the activation of divalent cation entry in rat parotid acinar cells, $[Ca^{2+}]_i$ could also have a direct regulatory role in the capacitative activation of divalent cation entry. The signalling mechanism from the internal pool to the plasma membrane could also be sensitive to $[Ca^{2+}]_i$. It remains to be established whether the retardation of carbachol stimulation of divalent cation entry in rat parotid acinar cells by elevated $[Ca^{2+}]_i$ is a result of effects of $[Ca^{2+}]_i$ on the divalent cation entry mechanism *per se* or on the capacitative activation of divalent cation entry.

We appreciate Dr. R.J. Turner's comments during the preparation of this manuscript. We also thank Drs. R.J. Turner, Ofer Eidelman, V.J. Horn, and T. Lockwich for helpful discussions during the course of this work.

References

1. Aub, D.L., Putney, J.W., Jr. 1984. Metabolism of inositol phosphates in parotid cells: Implications for the pathway of the phosphoinositide effect and for the possible messenger role of inositol triphosphate. *Life Sci.* **34:**1347–1355
2. Baum, B.J., Ambudkar, I.S., Helman, J., Horn, V.J., Melvin, J.E., Mertz, L.M., Turner, R.J. 1990. Dispersed salivary gland acinar cell preparations for use in studies of neuroreceptor coupled secretory events. *Methods Enzymol.* **192:**26–37
3. Baum, B.J., Ambudkar, I.S., Horn, V.J. 1991. Neurotransmitter regulation of calcium mobilization in salivary cells. *In:* The Biology of the Salivary Glands. K. Vergona, editor. (*in press*)
4. Berridge, M.J., Irvine, R.F. 1989. Inositol phosphates and cell signalling. *Nature* **341:**197–205
5. Bird, G., St J., Rossier, M.F., Hughes, A.R., Shears, S.B., Armstrong, D.L., Putney, J.W., Jr. 1991. Activation of Ca^{2+} entry into acinar cells by a non-phosphorylatable inositol triphosphate. *Nature* **352:**162–165
6. Dissing, S., Nauntofte, B., Sten-Knudsen, O. 1990. Spatial distribution of intracellular, free Ca^{2+} in isolated rat parotid acini. *Pfluegers Arch.* **417:**1–12
7. Foder, B., Scharff, O., Thastrup, O. 1989. Ca^{2+} transients and Mn^{2+} entry in human neutrophils induced by thapsigargin. *Cell Calcium* **10:**477–490
8. Foskett, J.K., Gunter-Smith, P.J., Melvin, J.E., Turner, R.J. 1989. Physiological localization of an agonist-sensitive pool of Ca^{2+} in parotid acinar cells. *Proc. Natl. Acad. Sci. USA* **86:**167–171
9. Hallam, T.J., Jacob, R., Merritt, J.E. 1988. Evidence that agonists stimulate bivalent-cation influx into human endothelial cells. *Biochem. J.* **255:**179–184
10. Horn, V.J., Baum, B.J., Ambudkar, I.S. 1988. β-adrenergic receptor stimulation induces inositol triphosphate production and Ca^{2+} mobilization in rat parotid acinar cells. *J. Biol. Chem.* **263:**12454–12460
11. Hoth, M., Penner, R. 1992. Depletion of intracellular Ca^{2+} stores activates a Ca^{2+} current in mast cells. *Nature* **355:**353–356
12. Hughes, A.R., Takemura, H., Putney, J.W., Jr. 1988. Kinetics of inositol 1,4,5-triphosphate and inositol cyclic 1 : 2,4,5-triphosphate metabolism in intact parotid acinar cells. *J. Biol. Chem.* **263:**10314–10319
13. Irvine, R.F. 1990. 'Quantal' Ca^{2+} release and the control of Ca^{2+} entry by inositol phosphates—a possible mechanism. *FEBS Lett.* **263:**5–9
14. Irvine, R.F., Anggard, E.E., Letcher, A.J., Downes, C.P. 1985. Metabolism of inositol 1,4,5-triphosphate and inositol 1,3,4-triphosphate in rat parotid glands. *Biochem. J.* **229:**505–511
15. Jacob, R. 1990. Agonist-stimulated divalent cation entry into single cultured umbilical vein endothelial cells. *J. Physiol.* **421:**55–77
16. Kasai, H., Augustine, G.J. 1990. Cytosolic Ca^{2+} gradients triggering unidirectional fluid secretion from exocrine pancreas. *Nature* **348:**735–738
17. Kass, G.E.N., Llopis, J., Chow, S.C., Duddy, S.K., Orrenius, S. 1990. Receptor-operated calcium influx in rat hepatocytes. *J. Biol. Chem.* **265:**17486–17492
18. Kwan, C.-Y., Putney, J.W., Jr. 1990. Uptake and intracellular sequestration of divalent cations in resting and methacholine-stimulated mouse lacrimal acinar cells. *J. Biol. Chem.* **265:**678–684
19. Loessberg, P.A., Zhao, H., Muallem, S. 1991. Synchronized oscillation of Ca^{2+} release in agonist-stimulated AR42J cells. *J. Biol. Chem.* **266:**1363–1366
20. Luckhoff, A., Clapham, D.E. 1992. Inositol 1,3,4,5,-tetrakisphosphate activates an endothelial Ca^{2+} permeable channel. *Nature* **355:**356–358
21. Marier, S.H., Putney, J.W., Jr., Van De Walle, C.M. 1978. Control of calcium channels by membrane receptors in the rat parotid gland. *J. Physiol.* **279:**141–151
22. Merritt, J.E., Rink, T.J. 1987. Regulation of cytosolic free Ca^{2+} in Fura-2 loaded rat parotid acinar cells. *J. Biol. Chem.* **262:**17362–17369
23. Merritt, J.E., Rink, T.J. 1987. The effects of substance P and carbachol on inositol tris- and tetrakisphosphate formation and cytosolic free calcium in rat parotid acinar cells. *J. Biol. Chem.* **262:**14912–14916
24. Mertz, L.M., Baum, B.J., Ambudkar, I.S. 1990. Refill status of the agonist-sensitive Ca^{2+} pool regulates Mn^{2+} influx into parotid acini. *J. Biol. Chem.* **265:**15010–15014
25. Mertz, L.M., Baum, B.J., Ambudkar, I.S. 1992. Membrane potential modulates divalent cation entry in rat parotid acini. *J. Membrane Biol.* **126:**183–193
26. Mertz, L.M., Horn, V.J., Baum, B.J., Ambudkar, I.S. 1990. Calcium entry in rat parotid acini: Activation by carbachol and aluminum fluoride. *Am. J. Physiol.* **258:**C654–661
27. Parker, I., Ivorra, I. 1990. Inhibition by Ca^{2+} of the inositol trisphosphate-mediated Ca^{2+} liberation: A possible mechanism for oscillatory release of Ca^{2+}. *Proc. Natl. Acad. Sci. USA* **87:**260–264

28. Pietri, F., Hilly,M., Mauger, J.-P. 1990. Calcium mediates the interconversion between two states of the liver inositol 1,4,5,triphosphate receptor. *J. Biol. Chem.* **265:**17478–17485
29. Petersen, O.H. 1989. Does inositol tetrakisphosphate play a role in the receptor-mediated control of calcium mobilization? *Cell Calcium* **10:**375–383
30. Petersen, O.H., Gallacher, D.V. 1988. Electrophysiology of pancreatic and salivary acinar cells. *Annu. Rev. Physiol.* **50:**65–80
31. Putney, J.W., Jr. 1986. A model for receptor-regulated calcium entry. *Cell Calcium* **7:**1–12
32. Sage, S.O., Merritt, J.E., Hallam, T.J., Rink, T.J. 1989. Receptor-mediated calcium entry in fura-2-loaded human platelets stimulated with ADP and thrombin. *Biochem. J.* **258:**923–926
33. Takemura, H., Hughes, A.R., Thastrup, O., Putney, J.W., Jr. 1989. Activation of calcium entry by the tumor promotor thapsigargin in rat parotid acinar cells. *J. Biol. Chem.* **264:**12266–12271
34. Takemura, H., Putney, J.W., Jr. 1989. Capacitative calcium entry in parotid acinar cells. *Biochem. J.* **258:**409–412
35. Taylor, C.W. 1990. Receptor-regulated Ca^{2+} entry: Secret pathway or secret messenger? *Trends Pharmacol. Sci.* **11:**269–271

Received 15 January 1992; revised 26 March 1992